



Optimizing of Wear Performance on Elevated Temperature of ZrO₂ Reinforced AMCs Using Weighted Superposition Attraction Algorithm

Dogan Simsek^{1*}, Dursun Ozyurek², Erol Ileri¹, Sener Akpınar³ and Aslan Deniz Karaoglan⁴

¹Department of Automotive Sciences, National Defense University, Balıkesir, 10100, Turkey

²Department of Manufacturing Engineering, Karabuk University, Karabuk, 78050, Turkey

³Department of Industrial Engineering, Dokuz Eylul University, Izmir, 35390, Turkey

⁴Department of Industrial Engineering, Balıkesir University, Balıkesir, 10145, Turkey

Received 02 March 2021; revised 21 March 2022; accepted 21 March 2022

In the current study, the zirconium oxide (ZrO₂) reinforced Aluminium Matrix Composites (AMCs) was designed as a brake lining and produced by mechanical alloying (MA) method. Wear tests of AMCs were performed according to ASTM G-99 at different sliding distance, operating temperatures and load in the range of 53 to 94 m, 20 to 340°C and 10 to 30 N respectively. Optimum wear performance parameters were determined using the Weighted Superposition Attraction (WSA) algorithm. Firstly, to formulize the problem as an optimization problem through the guidance of the regression modelling, an experimental design has been constructed, and the wear tests have been done at different reinforced rates, operating temperature and loads. Secondly, WSA algorithm has been adapted to tackle the formulated optimization problem. According to the results of WSA algorithm, the optimum rate of zirconium oxide (ZrO₂), load and operating temperature was determined as 12%, 206.33°C and 21.20 N respectively while keeping the friction coefficient between 0.15–0.24.

Keywords: Aluminium matrix composites, Hot Wear, Mechanical alloying, Zirconia reinforced composite

Introduction

Aluminium matrix composites (AMCs) have superior properties such as low density, high hardness, high specific strength, good corrosion resistance and good wear resistance.¹⁻³ Particle-reinforced AMCs are widely used in many industrial areas, especially in the automotive (brake system applications), aerospace and defence industries.⁴ In addition, AMCs stand out in properties such as high thermal and electrical conductivity. Therefore, the use of AMCs in the automotive industry is increasing day by day. Particle-reinforced AMCs improve the wear resistance of parts that work at momently increase or constantly high temperature such as internal combustion engine pistons, automotive and aircraft brakes.⁵ Ceramic particles used as a reinforcing element in particle reinforced AMCs can expand the thermal stability and operating temperature range of the matrix material.⁶ Wear resistance is an important parameter in many engineering fields. Many parameters such as material hardness, microstructure, the load it exposed during wear, working temperature, working environment,

working time and speed are the factors that affect the wear performance of the materials.⁷ In general, materials with high hardness have high wear resistance. However, hardness in AMCs varies according to the reinforcement amount added to the matrix material, distribution, and the size of the reinforcement material. In addition, when added more than a certain amount of reinforcement materials in the matrix, the hardness of AMCs increases, while their wear performance decreases due to breaks in service conditions. Ay *et al.* investigated the wear performance of in-situ TiAl₃ reinforced composite materials in which they added three different amounts (2% 4% and 6 wt%) of Ti (Titanium) and stated that the hardness increased with increasing Ti amount.¹ However, in the wear performance, they reported that in composites 4% and 6% Ti added they exhibit the same wear performance after a certain sliding distance. Increasing the amount of reinforcement in the matrix causes breaks in working conditions of AMC materials. In addition, the load to which the material is exposed during wear directly affects the wear resistance. Increasing the applied load increases the stresses on the tested material and the contact material contact surfaces. In many studies carried out under different loads, reported

*Author for Correspondence
E-mail: dsimsek@msu.edu.tr

weight loss increases with increasing applied load.^{8–10} In AMC exposed to the load, stress concentration occurs around reinforcement phase. With the effect of increased stress concentration, micro cracks formed (depending on time) on the contact surfaces of the particle-reinforced composites, proceedingly join-up of micro cracks and as a result debris occur (breaks) from the surface. In addition, another important factor is the operating temperatures. With the effect of increasing working temperature (as the material approaches recrystallization temperatures) the ductility of the material increases. Therefore, the wear resistance of AMCs decreases.^{5,11,12}

Going through the past studies, AMCs are generally known to have good wear behavior. In addition, the wear performances of these materials are determined within certain limits.^{13–15} However, determining all these limits at the same time requires a large amount of time and extra cost for researchers. Therefore, determination of optimum working conditions determines the working limits of the produced AMCs. These working conditions provide researchers that significant saving in terms of both time and cost. Metaheuristics can often find good solutions with less computational effort. Several meta-heuristic algorithms are proposed to search the feasible solution spaces. In the literature, diverse metaheuristic algorithms have been widely designed and used to solve various optimization problems.^{16–20} The Weighted Superposition Attraction (WSA) algorithm is a recently developed optimization algorithm taking place in the class of metaheuristics. In this study, to identify the optimum levels of reinforced rate, load, and operating temperature to minimize the weight loss and wear rate while keeping the friction rate between 0.15–0.24 the WSA algorithm has been implemented. When these purposes are considered, we can state that the current paper has two main contributions: formulating the problem as a constrained optimization problem and solving this problem as efficiently as possible through the WSA algorithm. In addition, its aimed is to determine the optimum load temperature and reinforcement amount in a certain friction coefficient range and contribute to future studies.

Materials and Methods

Material Processing and Experimental Procedure

Al-Si-Mg (A356) alloy powder was used as a matrix material in the experimental studies. ZrO₂ with an average powder size $\leq 10 \mu\text{m}$ was used as a

reinforcing material. In AMCs production, four different amounts (3%, 6%, 9% and 12 wt%) of reinforcement were added to the matrix. In addition, 2 wt% graphite was added as a solid lubricant to the matrix. The powders prepared were mechanically alloyed within a stainless-steel vial in a planetary type of mill. In the mechanical alloy, a fill rate of 50%, a ball powder ratio of 1:10, a milling time of 240 min, and as process control chemical (PCA) of 1 (wt.%) stearic acid were used. MA process was made in 15 min alloying and 10 min waiting periods to prevent overheating of the powders. MA composite powders were produced green compacts in $\text{Ø}12 \times 7$ mm dimension by pre-formed in steel mold with single axis hydraulic press (750 MPa). Zinc stearate was used as a lubricant in the cold forming (pressing) process of composite powders. The produced green compacts were sintered with 10–6 mbar vacuum, 5 °C/min heating speed, on 550°C operating temperature for 60 min in a vacuum heat treatment furnace. After sintering, the composites were cooled to room temperature in the furnace. Wear tests were carried out according to ASTM G-99 standard by using pin-on disc type standard wear test device. Three different sliding distance (53, 72 and 94 m), and five different operating temperatures (20, 100, 180, 260 and 340°C) were used in wear tests, including 0.5 m/s sliding speed and three different loads (10, 20 and 30 N). The sliding distances were determined to the stopping distances during braking of a car with different speeds.²¹ The operating temperatures were selected according to the maximum temperature formed due to friction between brake lining and disc during braking. In the wear tests was added a temperature module to the test device. Wear tests were started after the temperature module warmed up to the operating temperature and stabilized. Prior to the tests, the sample and disc surface were cleaned with ethanol. The spherical graphite cast iron as a counter disc was used in the wear tests. In every material group and at every temperature change, the counter disc was cleaned with 800 grit sandpaper with high-speed sanding device to ensure the same surface quality. The weight loss method was used to determine the wear in the composites. Each test was started at 0 m and weight loss was determined at the target distance. For determination of weight loss was used balance with a sensitivity of 1/10000 g. The weight loss, wear rate and friction coefficients in composites were calculated by taking the average of the data from 3 different samples from each AMC group.

Regression Modelling

This study formulates the relations between the factors (reinforced rate, load, and operating temperature) and the responses (weight loss, wear rate, and friction coefficient) through the calculated regression models mathematically. Then, the optimal or near-optimal factor levels those minimize the weight loss and wear rate under the constraint of having the friction coefficient a value from the interval of 0.15–0.24 are determined via the WSA algorithm by using the generated regression equations. The range in the friction coefficients used is according to the classes specified in “Road vehicles - Brake linings and pads for friction type brakes” TSE 555 (TSE 555, 1992)⁽²¹⁾ and “Friction Coefficient Identification and Environmental Marking System for Brake Linings (stabilized Mar 2019) J866_201903.”⁽²²⁾ Within the context of this current paper, the general full quadratic regression model represented in Eq. (1) has been used to formulize the mathematical relations between the factors and responses.

$$Y = \beta_0 + \sum_{k=1}^n \beta_k X_k + \sum_{k=1}^n \beta_{kk} X_k^2 + \sum_{k<l}^n \beta_{kl} X_k X_l + \varepsilon \dots (1)$$

β terms represent the regression coefficients; while Y is the response, k is the factor number X terms are the factors (X_k s are the linear terms, X_k^2 s are the quadratic terms, and X_{kk} s are the interaction terms), n is the total number of regression parameters, and ε is the residual error.²³ The matrix notation for this model may be written as:

$$Y = \beta X + \varepsilon \dots (2)$$

where, Y and X represent the output matrix (response values: weight loss, wear rate, and friction coefficient) and input matrix (factor values: reinforced rate, load, and operating temperature) respectively. Residuals are given by the ε matrix. β is a vector that is composed of the coefficients of the regression equation. β vector is calculated by using the Eq. (3).^(23,24)

$$\beta = (X^T X)^{-1} (X^T Y) \dots (3)$$

After calculating the regression equation, two statistical indicators are looked at to see if this equation can be used for optimization purposes. First one is the coefficient of determination (R^2). R^2 indicates how effective a regression model is in reflecting the dependent variables. For a successful formulation, R^2 calculated via Eq. (4) is expected to be closer to 1 (100%).

$$R^2 = \frac{\beta^T X^T Y - n \bar{Y}^2}{Y^T Y - n \bar{Y}^2} \dots (4)$$

If the R^2 is closer to 1, then this means that the factors used to model the response are adequate and there is no need to use additional factors at the regression model.²³ The second statistical indicator is the analysis of variance (ANOVA).²³ Hypothesis testing can also be useful for determining the importance of a regression model. There are two standard hypotheses. The first one is the H_0 (model is insignificant) and the other is H_1 (model is significant). The hypothesis testing is mainly performed to identify if the H_0 will be rejected or not. In line with this purpose, an appropriate and widely used method is the Analysis of Variance (ANOVA) that uses the p-value approach for decision making. H_0 is rejected when the p-value derived from the ANOVA analysis is less than the α (Type-I error), otherwise, H_1 is true and therefore the model is significant. In this study 95% confidence level is used, then this means the $\alpha = 1 - 0.95 = 0.05$.

Weighted Superposition Attraction (WSA) Algorithm

The WSA algorithm is a recently developed optimization algorithm which taking place in the class of metaheuristics. The algorithm originally designed by Baykasoglu & Akpinar to tackle complex continuous optimization problems.²⁵ The later implementations of the WSA algorithm have proved the algorithm's adequacy on tackling different optimization problems such as engineering design^{26–28}, binary optimization^{29,30}, resource constrained project scheduling.^{31–33}

The WSA algorithm combines the superposition principle and the attracted movement of agents while exploring the solution space of an optimization problem. At the initialisation phase, the WSA algorithm constructs a predefined number of solutions randomly. After that, the WSA algorithm constructs a single solution via the superposition principle as a target solution to direct all the other solutions towards it in comparison to their fitness values.²⁷ Before the start of this procedure, the WSA algorithm ranks the solutions on hand according to their fitness values and assigns weights to each solution on the basis of their ranks. To calculate these rank-based weights the WSA algorithm realizes a formula as follows: $weight(i) = i^{-\tau}$ where i is the rank of a solution and τ is a user defined parameter. The target solution determination procedure starts with an empty vector and turns it into a target solution iteratively as explained below. The procedure assigns priorities from the interval $[0, 1]$ to each digit of the empty

vector firstly. Then, the procedure compares the precalculated weights of each solution with these priorities of the empty vector's digits successively. If the procedure establishes a solution having a greater weight than the priority of the related digit of the initially empty vector, then, the procedure identifies the corresponding element of the related solution as a quotable candidate to the related empty position of the initially empty vector. This means, the procedure forms a candidate list for every digit of the initially empty vector.

After that, the procedure selects one element from the candidate list via roulette wheel to set as an element of the initially empty vector therefore the target solution. This procedure is ended when all the digits of the initially empty vector filled, namely a target solution was obtained. The next step of the WSA algorithm is to update the solutions on hand via the guidance of the constructed target solution. The WSA algorithm makes every solution to compare their fitness values against the target solution's fitness value. If the target solution is better than a solution, then the related solution is updated by moving it towards the constructed target solution. On the other hand, the WSA algorithm generates a random number from the interval $[0, 1]$ and compares it against the value calculated as $e^{(f(i)-f(tar))}$, where $f(i)$ is the fitness value of solution i and $f(tar)$ is the fitness value of target solution. If the randomly generated number is lower than or equal to the calculated value, then the related solution is also updated by moving it towards the target solution, otherwise, the related solution is updated by moving towards a randomly determined direction. The WSA algorithm updates each solution for its every dimension j ($1 \leq j \leq \mathcal{D}$) at iteration t via Eq. 5. Here, \mathcal{D} is the total number of decision variables of the related optimisation problem.

$$x_{ij}(t+1) = x_{ij}(t) + sl(t) * d_{ij}(t) * \|x_{ij}(t)\| \quad \dots (5)$$

where, $x_{ij}(t)$ refers to value of solution i on dimension j , $sl(t)$ is the step size, $d_{ij}(t)$ represents the move direction of solution i on its dimension j , $\|x_{ij}(t)\|$ denotes the distance between the value of solution i on its dimension j and the origin at t^{th} iteration, and $d_{ij}(t) \in \{-1, 0, 1\}$. In Eq. 6, the second term ($sl(t) * d_{ij}(t) * \|x_{ij}(t)\|$) of the right-hand-side realizes the update of a solution on a dimension and the WSA algorithm executes this update via the step sizing function given by Eq. 6.

$$sl(t+1) = \begin{cases} sl(t) - e^{-t/(t+1)} * \varphi * sl(t) & \text{if } r \leq \lambda \\ sl(t) + e^{-t/(t+1)} * \varphi * sl(t) & \text{if } r > \lambda \end{cases} \quad \dots (6)$$

As can be seen from Eq. 6, the step sizing function requires an initial step size $sl(0)$ to be set and the WSA algorithm updates this step size proportionally throughout the iterations. This update uses a random number r from the interval $[0, 1]$ and the user defined parameters λ (*Lambda*) and φ (*Phi*). More detailed information about the general framework of the WSA algorithm and its steps can be obtained from Baykasoğlu & Akpınar.^{25,27}

Results and Discussions

Wear Test Results

The response surface results of weight loss versus reinforced rate and load are depicted in Fig. 1a. It is observed that the weight loss increases with increasing load and decreases with increasing amount of reinforcement in the matrix which improves the resistance against plastic deformation and the hardness and wear resistance of the material.³⁴ Past study reports that increased reinforcement in the matrix improves hardness and wear resistance.³⁵

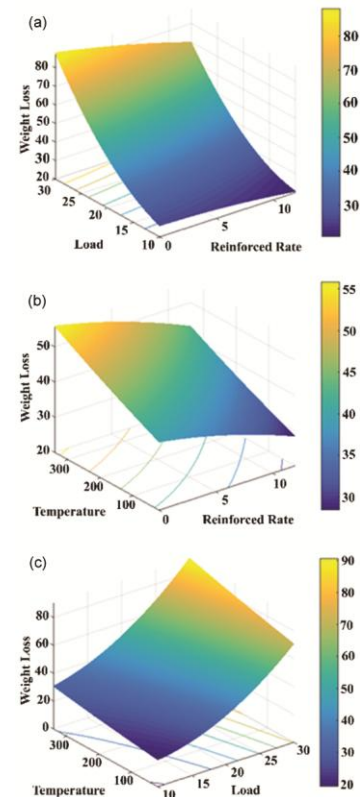


Fig. 1 — Response surface results of weight loss versus a) Reinforced rate and load, b) Reinforced rate and temperature and c) Load and temperature

Increasing load increases the stress on the sample contact surface, and this increases the particles broken off from the surface and causes an increase in weight loss. The response surface results of weight loss as a function of amount of reinforcement and temperature are shown in Fig. 1b. It can be seen in Fig. 1b that the weight loss increases with increasing temperature and decreases with increasing amount of reinforcement in the matrix. The highest weight loss was measured for the matrix (Al-2% G) at 340°C and the lowest weight loss was measured for the composite (12% ZrO₂) at 20°C. Increasing operating temperature increases the ductility of the matrix and decreases the strength.³⁶ Therefore, the weight loss of composites increased at high working temperatures.^{37,38} Similarly, Fig. 1c depicts the weight loss response surface results versus load and temperature. As seen in Fig. 1c, the weight loss increases with increasing working temperature and load. It is understood that the applied load is more effective than the operating temperature on the weight loss of the composites produced. The matrix ductility increases with increasing operating temperature and load. Increasing stress in the wear surface and sub-surface ignite to develop micro cracks. Micro cracks progress easily and combine to produce macro cracks at high load and operating temperatures. Zhu *et al.* reports that the wear resistance of the composites decreases by the increasing load and operating temperature.³⁹

From the response surface results of wear rate as a function of reinforcement rate and load as shown in Fig. 2a, wear rate decreases with increasing amount of reinforcement rate for all loads. Increasing amount of reinforcement in the matrix increases the strength of the composites.⁴⁰ Increasing the amount of reinforcement in the matrix provides a shared response to the load by both the matrix and reinforcement, and this decrease the weight loss and wear ratio. The graph also shows that the wear rate is high especially at low and high loads (10 N and 30 N). At low loads, parts breaking off on the sample surface can easily go away from the tribological system which increases the wear rate. Similarly, at high loads, high stress developed in the sample worn surface increases the weight loss and wear rate. Similar results were observed by Kumar *et al.*³⁷ The response surface results of wear rate versus reinforcement rate and operation temperature are shown in Fig. 2b. As can be seen in Fig. 2b, wear rate decreases with increasing reinforcement rate at all operating temperatures. Also, as the operation

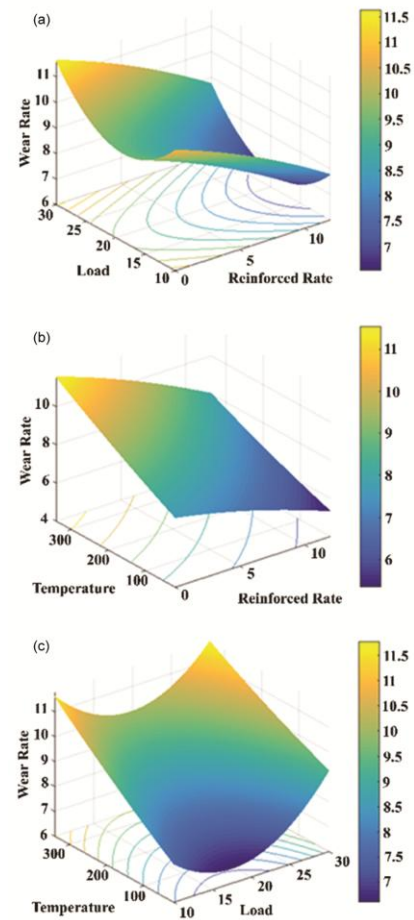


Fig. 2 — Response surface results of wear rate versus a) Reinforced rate and load, b) Reinforced rate and temperature and c) Load and temperature

temperature increases, the wear rate increases at all loads. Wear rates also support the wear loss results as expected. The strength of the material decreases with increasing operation temperature and it causes increasing in wear rate and weight loss.³⁶

The response surface results of friction coefficient as a function of the reinforcement rate and load are given in Fig. 3a. Obtained results show that the friction coefficient decreases at all loads with increasing amount of reinforcement in the matrix. The highest friction coefficient was measured in the matrix at 30 N load. Increasing reinforcement rate in the matrix increases the hardness which causes decreasing in friction coefficient. Similar results were observed by Simsek *et al.*³⁵, Uyyuru *et al.*⁴¹ and Çelik *et al.*⁴² The response surface results of friction coefficient as a function of reinforcement rate and temperature are given in Fig. 3b. As seen in Fig. 3b, the friction coefficient increases with increasing operating temperature. Increasing of ductility of the

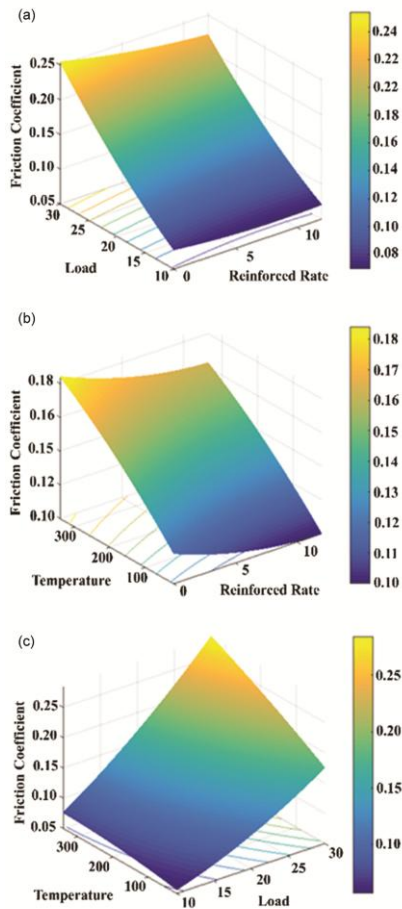


Fig. 3 — Response surface results of friction coefficient
 a) Reinforced rate and load b) Reinforced rate and temperature
 c) Load and temperature

matrix at high temperatures decreases the strength of the material. Wear particles that break off the sample surface during the wear test smear on the surface and this lead to increase the surface roughness, causing an increase of friction coefficient.^{6,43} The response surface results of friction coefficient as a function of the temperature and load are given in Fig. 3c. Results show that the friction coefficient increases with increasing load and temperature. It was observed that the highest friction coefficient is measured at the highest operating temperature for all loads. The material strength decreases, and the surface roughness increases with increase in operating temperature, and this leads to the increase in friction coefficient.

In Fig. 4, the SEM images of the worn surface of 12% ZrO_2 reinforced AMC materials at different temperatures are shown. It further demonstrates the deformation on the sample surface increases with increasing in the operation temperature. Worn surface SEM images (Fig. 4a) of the composite tested at room temperature show deformation tracks and parallel spalling to the sliding direction on the surface. In the worn surface obtained at 100°C temperature, micro cracks and micro chipping smeared on the surface are observed. Also, there are worn particles smeared on the surface. At higher operating temperatures, parallel grooves to the slide direction on the surface are observed. When the temperature reaches 260°C and 340°C (Figs 4d and 4e), there are more micro cracks and spalling than those of at lower temperatures (Figs

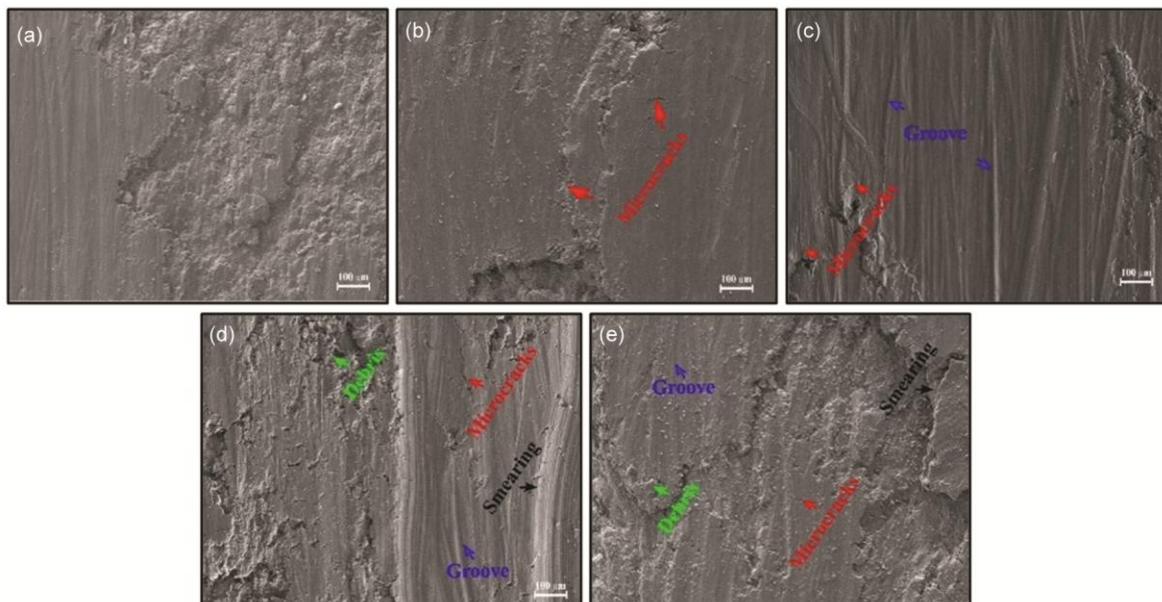


Fig. 4 — SEM images of worn surfaces in different temperature under 30 N loads of composite materials the 12% ZrO_2 contain at:
 a) Room Temperature, b) 100°C, c) 180°C, d) 260°C, e) 340°C

4 a–c). Stress concentrations caused by higher temperature and higher load leads to micro cracks as the slide distance increases.⁴⁴ The presence of micro cracks on the surface weakens the bond between the reinforcing material and the matrix and allows the micro cracks to progress more easily which leads to macro cracks just beneath the wear surface and spalling on the wear surface.⁴⁵ Similar results were observed by Simsek *et al.*⁴³

WSA Results

The main goal of this current paper is to optimize the objectives of weight loss and wear rate under the friction coefficient constraint. The reinforced rate, load, and operating temperature have been identified as the factors affecting these objectives. In line with this purpose, the regression models have been formulized firstly and then an optimization problem has been developed thanks to these models. After that, this paper has aimed to optimize this problem via the WSA algorithm. The aforementioned factors with their actual and coded levels are represented Table 1.

With the guidance of the factor levels depicted in Table 1, an experimental design has been created and the related experiments have been executed. The experimental results are presented in Table 2. The formulas exposing the relations between the independent and dependent variables have been obtained as the second-order regression forms from a small number of observations of the responses provided by the experimental setup. To ensure the clarity for the readers, the regression equations have been formulized by using the observed factor levels due to the actual factor levels. However, for a successful implementation of the WSA algorithm, we preferred to use formulas determined with the guidance of the coded factors. In this study, the handled problem is a multi-objective optimization since the aim is to minimize the weight loss and wear rate simultaneously under the constraint of having a friction coefficient from the interval of 0.15–0.24. To optimize this multi-objective problem via the WSA algorithm, the coded responses have been used as stated before. For this purpose, each column has been

divided by that column's highest observation value. We present the regression equations with uncoded values for the readers; however, in the background for the WSA algorithm, models were used for coded factor levels and responses. The R^2 and ANOVA do not change. The R^2 values of the regression models have been determined through the ANOVA analyses done via MINITAB 16 statistical package. For the optimization phase, we have coded the WSA algorithm in MATLAB (R2019b) and obtained the results by running the algorithm on a personal computer having Intel Core i7 – 2.2 GHz processor and 8 GB RAM. As a result of the experimental design of the uncoded units calculated via Eqs (1–3), the second-order polynomial regression models (full quadratic models) given by Eqs (7–9) have been obtained.

$$Weight\ Loss = 20.7638754164 + 0.5641020314X_1 - 1.09713865X_2 + 0.0181747068X_3 - 0.0329226984X_1^2 + 0.09909935X_2^2 + 0.0000183594X_3^2 - 0.0536098056X_1X_2 - 0.0004502205X_1X_3 + 0.0013385625X_2X_3 \quad \dots (7)$$

$$Wear\ Rate = 12.4213204603 - 0.1198146448X_1 - 0.5888937542X_2 + 0.0154853667X_3 - 0.0059092769X_1^2 + 0.0169673367X_2^2 + 0.0000043542X_3^2 + 0.00022175X_1X_2 - 0.0003147201X_1X_3 - 0.0002424306X_2X_3 \quad \dots (8)$$

$$Fric.\ Coef. = 0.0307745079 - 0.0007708502X_1 + 0.0018605417X_2 - 0.0000177562X_3 + 0.0001207319X_1^2 + 0.0001115667X_2^2 - 0.000000153X_3^2 - 0.0001077778X_1X_2 - 0.000000892X_1X_3 + 0.0000140063X_2X_3 \quad \dots (9)$$

The R^2 statistics (R^2 , R^2 -Prediction, R^2 -Adjusted) associated with the given models for the responses have been calculated via MINITAB-16. The results for R^2 statistics are summarized in Table 3.

From the observation of the data given in Table 3, it can be clearly seen that the formulized regression models satisfactorily reflect the dependent variables due to the R^2 values close to 100%. The factors of namely reinforced rate, load, and operating temperature have been successfully realized to model the mentioned responses. The significance of the formulized regression models (Eqs (7–9)) can be clearly seen from the ANOVA results represented in Table 4. Due to the p-values lower than alpha (5%) the alternative hypothesis (H_1) is accepted, and this situation correspond to the significant regression models and by this means these models can be used for the optimization purpose.

Table 1 — Factors list of actual and corresponding coded values of reinforced rate, load, and operating temperature

Factor	Symbol abbreviation	Level	Level		
			-1	0	1
Reinforced rate (wt%)	RR	X_1	0	6	12
Load (N)	L	X_2	10	20	30
Temperature (°C)	T	X_3	20	180	340

Table 2 — Design of experiments and observed responses

Run No.	Original factor levels			Coded factor levels			Weight loss	Wear rate	Friction coefficient
	X ₁	X ₂	X ₃	X ₁	X ₂	X ₃	Y _{i1}	Y _{i2}	Y _{i3}
1	0	10	20	-1	-1	-1	20.6000	8.2729	0.0595
2	0	10	180	-1	-1	0	26.9000	10.8020	0.0733
3	0	10	340	-1	-1	1	35.1000	14.0960	0.0815
4	0	20	20	-1	0	-1	36.8000	7.3894	0.1233
5	0	20	180	-1	0	0	44.6000	8.9556	0.1477
6	0	20	340	-1	0	1	55.2000	11.0841	0.1919
7	0	30	20	-1	1	-1	79.3000	10.6155	0.1900
8	0	30	180	-1	1	0	93.3333	12.4941	0.2610
9	0	30	340	-1	1	1	98.2000	13.1456	0.3060
10	3	10	20	-1	-1	-1	18.9667	7.4897	0.0590
11	3	10	180	-1	-1	0	26.0000	10.2670	0.0727
12	3	10	340	-1	-1	1	31.2330	12.3330	0.0798
13	3	20	20	-1	0	-1	35.3333	6.9764	0.1121
14	3	20	180	-1	0	0	45.1333	8.9113	0.1465
15	3	20	340	-1	0	1	53.2333	10.5106	0.1778
16	3	30	20	-1	1	-1	76.7667	10.1048	0.1830
17	3	30	180	-1	1	0	84.6000	11.1359	0.2470
18	3	30	340	-1	1	1	90.5000	11.9125	0.2890
19	6	10	20	0	-1	-1	21.2667	8.2721	0.0584
20	6	10	180	0	-1	0	23.7000	9.2180	0.0719
21	6	10	340	0	-1	1	31.0000	12.0580	0.0804
22	6	20	20	0	0	-1	33.1000	6.4374	0.1077
23	6	20	180	0	0	0	43.1333	8.3888	0.1422
24	6	20	340	0	0	1	56.0000	10.8911	0.1621
25	6	30	20	0	1	-1	68.5333	8.8858	0.1760
26	6	30	180	0	1	0	79.7000	10.3336	0.2320
27	6	30	340	0	1	1	85.8000	11.1245	0.2890
28	9	10	20	1	-1	-1	18.6000	7.1254	0.0569
29	9	10	180	1	-1	0	22.2000	8.5040	0.0710
30	9	10	340	1	-1	1	25.7660	9.8700	0.0774
31	9	20	20	1	0	-1	32.0667	6.1422	0.1010
32	9	20	180	1	0	0	38.0000	7.2786	0.1376
33	9	20	340	1	0	1	48.3333	9.2579	0.1631
34	9	30	20	1	1	-1	70.8667	9.0493	0.1670
35	9	30	180	1	1	0	77.1000	9.8453	0.2190
36	9	30	340	1	1	1	90.7000	11.5820	0.2660
37	12	10	20	1	-1	-1	16.6330	6.2526	0.0566
38	12	10	180	1	-1	0	21.2660	7.9940	0.0692
39	12	10	340	1	-1	1	23.7000	8.9090	0.0741
40	12	20	20	1	0	-1	30.6000	5.7515	0.0949
41	12	20	180	1	0	0	35.3333	6.6411	0.1366
42	12	20	340	1	0	1	45.3333	8.5207	0.1596
43	12	30	20	1	1	-1	56.9667	7.1381	0.1660
44	12	30	180	1	1	0	65.6000	8.2199	0.2270

Table 3 — Calculated R² values

Response	R ² (%)	R ² (predicted) (%)	R ² (adj) (%)
Weight loss	99.04	98.35	98.79
Wear rate	94.83	90.54	93.49
Friction coefficient	99.67	99.41	99.59

Table 4 — ANOVA results for the regression models

Response	Symbol	P-Value vs Alpha	Result
Weight loss	\hat{Y}_1	0.000 < 0.05	Model significant
Wear rate	\hat{Y}_2	0.000 < 0.05	Model significant
Friction coefficient	\hat{Y}_3	0.000 < 0.05	Model significant

When the ranges of design parameters are considered, it is obvious that the regression equations formulized for the responses of weight loss, wear rate, and friction coefficient have satisfactory levels of accuracy. The performances of the formulized models are clarified in Table 5. The reader must be aware that

the Y_i is depicted the observed responses while \hat{Y}_i is depicted the expected results calculated through the formulized regression equations. Additionally, PE_{i1} , PE_{i2} and PE_{i3} , which are calculated by the formula given in Eq. (10), refers to the prediction error of the i th run.

Table 5— Performance tests for the regression equations

Run No. (i)	Original factor levels			Weight loss			Wear rate			Friction coefficient		
	X_1	X_2	X_3	Y_{i1}	\hat{Y}_{i1}	PE_{i1} (%)	Y_{i2}	\hat{Y}_{i2}	PE_{i2} (%)	Y_{i3}	\hat{Y}_{i3}	PE_{i3} (%)
1	0	10	20	20.6000	20.34097	1.27	8.2729	8.492079	2.58	0.0595	0.062922	5.44
2	0	10	180	26.9000	25.97813	3.55	10.8020	10.72118	0.75	0.0733	0.077594	5.53
3	0	10	340	35.1000	32.55528	7.82	14.0960	13.17322	7.00	0.0815	0.084432	3.47
4	0	20	20	36.8000	39.36711	6.52	7.3894	7.644857	3.34	0.1233	0.117798	4.66
5	0	20	180	44.6000	47.14596	5.40	8.9556	9.486071	5.59	0.1477	0.154881	4.64
6	0	20	340	55.2000	55.86482	1.19	11.0841	11.55022	4.04	0.1919	0.184128	4.20
7	0	30	20	79.3000	78.21311	1.39	10.6155	10.1911	4.16	0.1900	0.194988	2.56
8	0	30	180	93.3333	88.13366	5.90	12.4941	11.64443	7.30	0.2610	0.254481	2.56
9	0	30	340	98.2000	98.99422	0.80	13.1456	13.32068	1.31	0.3060	0.306138	0.05
10	3	10	20	18.9667	20.10167	5.65	7.4897	8.067221	7.16	0.0590	0.058409	1.01
11	3	10	180	26.0000	25.52272	1.87	10.2670	10.14526	1.20	0.0727	0.072653	0.06
12	3	10	340	31.2330	31.88377	2.04	12.3330	12.44623	0.91	0.0798	0.079062	0.93
13	3	20	20	35.3333	37.51951	5.83	6.9764	7.226651	3.46	0.1121	0.110052	1.87
14	3	20	180	45.1333	45.08225	0.11	8.9113	8.916799	0.06	0.1465	0.146706	0.13
15	3	20	340	53.2333	53.585	0.66	10.5106	10.82988	2.95	0.1778	0.175526	1.28
16	3	30	20	76.7667	74.75721	2.69	10.1048	9.779548	3.33	0.1830	0.184009	0.55
17	3	30	180	84.6000	84.46166	0.16	11.1359	11.08181	0.49	0.2470	0.243073	1.62
18	3	30	340	90.5000	95.10611	4.84	11.9125	12.607	5.51	0.2890	0.294302	1.80
19	6	10	20	21.2667	19.26975	10.36	8.2721	7.535996	9.77	0.0584	0.056069	4.16
20	6	10	180	23.7000	24.4747	3.17	9.2180	9.462968	2.59	0.0719	0.069885	2.88
21	6	10	340	31.0000	30.61964	1.24	12.0580	11.61287	3.83	0.0804	0.075866	5.98
22	6	20	20	33.1000	35.0793	5.64	6.4374	6.702079	3.95	0.1077	0.104479	3.07
23	6	20	180	43.1333	42.42594	1.67	8.3888	8.241161	1.79	0.1422	0.140705	1.03
24	6	20	340	56.0000	50.71258	10.43	10.8911	10.00318	8.88	0.1621	0.169096	4.11
25	6	30	20	68.5333	70.70871	3.08	8.8858	9.261628	4.06	0.1760	0.175202	0.46
26	6	30	180	79.7000	80.19705	0.62	10.3336	10.41282	0.76	0.2320	0.233838	0.79
27	6	30	340	85.8000	90.6254	5.32	11.1245	11.78695	5.62	0.2890	0.28464	1.53
28	9	10	20	18.6000	17.84523	4.23	7.1254	6.898404	3.29	0.0569	0.055903	1.78
29	9	10	180	22.2000	22.83407	2.78	8.5040	8.67431	1.96	0.0710	0.06929	2.47
30	9	10	340	25.7660	28.76291	10.42	9.8700	10.67315	7.52	0.0774	0.074844	3.42
31	9	20	20	32.0667	32.04648	0.06	6.1422	6.071139	1.17	0.1010	0.101079	0.09
32	9	20	180	38.0000	39.17702	3.00	7.2786	7.459156	2.42	0.1376	0.136877	0.56
33	9	20	340	48.3333	47.24756	2.30	9.2579	9.070106	2.07	0.1631	0.16484	1.07
34	9	30	20	70.8667	66.0676	7.26	9.0493	8.637341	4.77	0.1670	0.168569	0.93
35	9	30	180	77.1000	75.33984	2.34	9.8453	9.637469	2.16	0.2190	0.226777	3.43
36	9	30	340	90.7000	85.55207	6.02	11.5820	10.86053	6.64	0.2660	0.27715	4.02
37	12	10	20	16.6330	15.8281	5.09	6.2526	6.154445	1.59	0.0566	0.057909	2.26
38	12	10	180	21.2660	20.60083	3.23	7.9940	7.779285	2.76	0.0692	0.070869	2.35
39	12	10	340	23.7000	26.31356	9.93	8.9090	9.627059	7.46	0.0741	0.075994	2.49
40	12	20	20	30.6000	28.42105	7.67	5.7515	5.333832	7.83	0.0949	0.099853	4.99
41	12	20	180	35.3333	35.33549	0.01	6.6411	6.570784	1.07	0.1366	0.135222	1.04
42	12	20	340	45.3333	43.18992	4.96	8.5207	8.030668	6.10	0.1596	0.162757	1.97
43	12	30	20	56.9667	60.83388	6.36	7.1381	7.906687	9.72	0.1660	0.164109	1.15
44	12	30	180	65.6000	69.89001	6.14	8.2199	8.755749	6.12	0.2270	0.221889	2.30

$$PE_i = \frac{Y_i - \hat{Y}_i}{\hat{Y}_i} = \frac{\varepsilon_i}{\hat{Y}_i} \quad \dots (10)$$

The confirmation tests for the regression equations are presented in Table 6. In this table, the performance of the models is given for different factor values that were not used when calculating the regression models.

Results presented in Table 6 indicate that the regression models are able to reflect the given observations with the prediction errors (PE) less than 8%. In the second stage of this paper, we have firstly modelled the problem as a constrained continuous optimization problem (by using the preidentified regression Eqs (7–9) as given below.

$$\text{Min Weight Loss} + \text{Wear Rate} \quad \dots (11)$$

s.t.

$$\text{s.t. } 0.15 \leq \text{Friction Coefficient} \leq 0.24; \quad X_1 \in [0, 12]; \\ X_2 \in [10, 30]; \quad X_3 \in [20, 340] \quad \dots (12)$$

Secondly, we used the WSA algorithm to tackle the problem. Since the problem is a constrained optimization problem, the WSA algorithm requires a constraint handling mechanism to prevent the algorithm to result in infeasibility. Therefore, the ITCH approach^{27,46,47} was adapted to the WSA algorithm. Additionally, the values of the control parameters of the WSA algorithm with their definitions are given in Table 7. All the values given in Table 6 were determined through a set of preliminary experiments. The confirmations for the optimization results are given in Table 8.

Optimization results obtained for load and temperature in the model proposed in the study are as

Table 6 — Confirmation tests for the regression equations

Run No. (i)	Original factor levels			Weight loss			Wear rate			Friction coefficient		
	X ₁	X ₂	X ₃	Y _{i1}	\hat{Y}_{i1}	PE _{i1} (%)	Y _{i2}	\hat{Y}_{i2}	PE _{i2} (%)	Y _{i3}	\hat{Y}_{i3}	PE _{i3} (%)
1	0	10	100	24.6000	23.04205	6.76	10.2230	9.578764	6.73	0.0668	0.071237	6.23
2	0	10	260	30.1830	29.14921	3.55	12.1210	11.91933	1.69	0.0762	0.081992	7.06
3	0	20	100	40.9000	43.13903	5.19	8.2127	8.537597	3.81	0.1392	0.137319	1.39
4	0	20	260	53.2333	51.38789	3.59	10.6892	10.49028	1.90	0.1736	0.170484	1.80
5	0	30	100	84.9667	83.05588	2.30	11.3741	10.8899	4.45	0.2290	0.225714	1.46
6	0	30	260	96.2000	93.44644	2.95	12.8779	12.45469	3.40	0.2720	0.281289	3.30
7	3	10	100	24.2660	22.69469	6.92	9.5826	9.078373	5.55	0.0686	0.06651	3.14
8	3	10	260	28.0660	28.58574	1.82	11.0830	11.26788	1.64	0.0760	0.076837	1.09
9	3	20	260	51.4000	49.21613	4.44	10.1486	9.845474	3.08	0.1636	0.162095	0.91
10	3	30	100	80.8000	79.49194	1.65	10.6357	10.40281	2.24	0.2160	0.21452	0.69
11	6	10	260	27.7000	27.42967	0.99	10.7740	10.51005	2.51	0.0778	0.073855	5.34
12	6	20	260	48.7000	46.45176	4.84	9.4714	9.094303	4.15	0.1515	0.15588	2.84
13	9	10	100	21.2000	20.22215	4.84	8.1210	7.75849	4.67	0.0669	0.063576	5.23
14	9	10	260	24.7730	25.68099	3.54	9.4740	9.645863	1.78	0.0756	0.073046	3.50
15	9	20	100	34.9333	35.49425	1.58	6.6912	6.737281	0.68	0.1233	0.119957	2.76
16	9	20	260	40.9000	43.09479	5.09	7.8341	8.236764	4.89	0.1477	0.151838	2.74
17	9	30	100	74.8333	70.58622	6.02	9.5559	9.109538	4.90	0.2030	0.198652	2.19
18	12	10	100	18.9330	18.09697	4.62	7.1170	6.938999	2.57	0.0641	0.065368	1.94
19	12	10	260	24.3000	23.3397	4.11	9.1340	8.675306	5.29	0.0748	0.074411	0.52
20	12	20	100	31.6000	31.76077	0.51	6.3452	5.924441	7.10	0.1200	0.118517	1.24

Table 7 — Parameters with their values of the WSA algorithm

Parameter	Definition	Value	Parameter	Definition	Value
MaxIter	Maximum number of iterations	50000	λ	User defined parameter	0.75
NS	Number of solutions at each iteration	50	φ	User defined parameter	0.0001
τ	User defined parameter	0.8	sl ₀	Initial step size	0.001

Table 8 — Confirmations for the optimization results

Response	Reinforced Rate (X ₁)	Load (X ₂)	Temperature (X ₃)	(Y _i)	WSA (\hat{Y}_i)	PE (%)
Weight loss	12	21.205289	206.334328	40.4739±3.12	39.7205	1.9
Wear rate	12	21.205289	206.334328	7.2765±1.016	6.8715	5.9
Friction coefficient	12	21.205289	206.334328	0.1507±0.0012	0.1500	0.5

given in Table 8. However, in the confirmation tests, was used as load 21.2 N and temperature $206.3 \pm 1^\circ\text{C}$ due to the test device sensitivity. The results given in Table 8 represents that formulized constrained continuous problem is an effective tool to optimize slot design parameters due to the prediction errors at most 5.9%. According to the obtained results, we can strongly conclude that the WSA algorithm has an effective prediction performance in solving the modelled constrained continuous optimization problem. We can also claim that the WSA algorithm is able to produce accurate predictions for the problem on hand. Additionally, an average CPU time of 24.9834 seconds confirms the effectiveness of the WSA algorithm in terms of execution time. In the literature, it is reported that the optimum parameters are determined with low error rates for maximum wear resistance in studies conducted with different optimization methods.^{48–50}

Conclusions

In the current study, we have dealt with determination of the wear performance parameters to minimize the weight loss and wear rate while keeping the friction rate between 0.15–0.24. A constrained continuous optimization model has been developed for the related problem through the guidance of the regression modelling and after that, this optimization problem has been solved via the WSA algorithm. The main goal of the WSA algorithm was to find the optimal or near-optimal wear performance parameters namely operation temperature and load, and rate of zirconium oxide (ZrO_2) in aluminium matrix composites (AMCs). Empirical relationships between the wear performance parameters and the responses have been derived through the regression modelling. Then, by using these regression models, we were able to formulate the problem as an optimization model through which we could tackle the problem via the WSA algorithm. The parameters namely reinforced rate, load and operating temperature were optimised using the desirability based WSA algorithm to minimise the weight loss and wear rate while keeping the friction coefficient between 0.15–0.24. For AMCs, minimum weight loss and wear rate predicted was 40.47 g and $7.27 \times 10^{-3} \text{ mm}^3/\text{Nm}$ respectively at a rate of 12% ZrO_2 , load of 21.20 N and operating temperature of 206.33°C . Confirmation test results given in Table 8 confirmed these findings and the effectiveness of the designed WSA algorithm. It further predicts an error of weight loss and wear rate

of 1.9% and 5.9% respectively. These results indicate that WSA algorithm performed slightly better results for the responses focused within the context of this paper. In addition, in this study, it was seen that the amount of reinforcement, load and temperature parameters of the composite materials, which are desired to work in the desired friction coefficient range from D class friction materials according to the TSE 555 standard, can be determined with a very low error rate.

References

- 1 Ay H, Ozyurek D, Yildirim M & Bostan B, The effects of B4C amount on hardness and wear behaviours of 7075-B4C composites produced by powder metallurgy method, *Acta Phys Pol A*, **129(4)** (2016) 565–568.
- 2 Nie J, Wang F, Chen Y, Mao Q, Yang H, Song Z, Liu X & Zhao Y, Microstructure and corrosion behavior of Al-TiB2 /TiC composites processed by hot rolling, *Results Phys*, **14** (2019) 1–7.
- 3 Şimşek I, Yildirim M, Özyürek D & Simsek D, Basınçsız infiltrasyon yöntemiyle üretilmiş SiO_2 takviyeli alüminyum kompozitlerin aşınma davranışlarının incelenmesi, *Politeknik Dergisi*, **22(1)** (2019) 81–85
- 4 Mallireddy N & Siva K, Investigation of microstructural, mechanical and corrosion properties of AA7010-TiB2 in-situ metal matrix composite, *Sci Eng Compos Mater*, **27(1)** (2020) 97–107.
- 5 Rajaram G, Kumaran S, Srinivasa T & Kamaraj M, Studies on high temperature wear and its mechanism of Al-Si/graphite composite under dry sliding conditions, *Tribol Int*, **43** (2010) 2152–2158.
- 6 Simsek D & Ozyurek D, The wear performance at high temperatures of ZrO_2 reinforced aluminum matrix composites produced by mechanochemical reaction method, *J Tribol*, **142(10)** (2020) 101701.
- 7 Varga M, Winkelmann H & Badisch E, Impact of microstructure on high temperature wear resistance, *Procedia Eng*, **10** (2011) 1291–1296.
- 8 Ozyurek D, Tekeli S, Gural A, Meyveci A & Guru M, Effect of Al_2O_3 amount on microstructure and wear properties of Al- Al_2O_3 metal matrix composites prepared using mechanical alloying method, *Powder Metall Metal Ceram*, **49(5-6)** (2010) 289–294.
- 9 Uthayakumar M, Aravindan S & Rajkumar K, Wear performance of Al-SiC-B4C hybrid composites under dry sliding conditions, *Mater Des*, **47** (2013) 456–464.
- 10 Singh J & Chauhan A, Overview of wear performance of aluminium matrix composites reinforced with ceramic materials under the influence of controllable variables, *Ceram Int*, **42(1)** (2016) 56–81.
- 11 Raju R S S, Panigrahi M K, Ganguly R I & Rao G S, Tribological behaviour of Al-1100-coconut shell ash (CSA) composite at elevated temperature, *Tribol Int*, **129** (2019) 55–66.
- 12 Nemati N, Emamy M, Penkov O V, Kim J & Kim D E, Mechanical and high temperature wear properties of extruded Al composite reinforced with $\text{Al}_{13}\text{Fe}_4$ CMA nanoparticles, *Mater Des*, **90** (2016) 532–544.

- 13 Ozyurek D & Tekeli S, An investigation on wear resistance of SiCp-reinforced aluminum composites produced by mechanical alloying, *Sci Eng Compos Mater*, **17(1)** (2010) 31–38.
- 14 Ozyurek D, Kalyon A, Yildirim M, Tuncay T & Ciftci I, Experimental investigation and prediction of wear properties of Al/SiC metal matrix composites produced by thixomoulding method using Artificial Neural Networks, *Mater Des*, **63** (2014) 270–277.
- 15 Li J C, Lin X, Kang N, Lu J L, Wang Q Z & Huang W D, Microstructure, tensile and wear properties of a novel graded Al matrix composite prepared by direct energy deposition, *J Alloy Compoun*, **826** (2020) 154077.
- 16 Pandiyan A, Arun K G, Ranganthan S & Madhu S, Optimization of wear performance on aluminium die cast A360-M1 master alloy using response surface method, *Mater Today: Proceed*, **22** (2020) 551–557.
- 17 Wang C, Ming K J, Yu T, Gang X N & Hao C K, Material and shape optimization of bi-directional functionally graded plates by GIGA and an improved multi-objective particle swarm optimization algorithm, *Comput Methods Appl Mech Eng*, **366** (2020) 113017.
- 18 Nwobi-okoye C C, & Ochieze B Q, Age hardening process modeling and optimization of aluminum alloy A356/Cow horn particulate composite for brake drum application using RSM, ANN and simulated annealing, *Def Technol*, **14** (2018) 336–345.
- 19 Hage R, Hage I, Ghnatios C, Jawahir I S & Hamade R, Optimized tabu search estimation of wear characteristics and cutting forces in compact core drilling of basalt rock using PCD tool inserts, *Comput Ind Eng*, **136** (2019) 477–493.
- 20 Singh R, Shadab M & Rai R N, Optimization of machining process parameters in conventional turning operation of Al5083/B4C composite under dry condition, *Mater Today: Proceed*, **5** (2018) 19000–19010
- 21 Road vehicles - Brake linings and pads for friction type brakes, <https://intweb.tse.org.tr/standard/standard/Standard.aspx?> [accessed February 2022]
- 22 Friction Coefficient Identification and Environmental Marking System for Brake Linings (stabilized Mar 2019) J866_201903, https://www.sae.org/standards/content/j866_201903/ [accessed February 2022].
- 23 Montgomery D C, *Design and analysis of experiments* (John Wiley & Sons, New Jersey–Hoboken) 2013.
- 24 Mason R L, Gunst R F & Hess J L, *Statistical Design and Analysis of Experiments* (John Wiley & Sons Inc: New Jersey) 2003.
- 25 Baykasoğlu A & Akpınar Ş, Weighted superposition attraction (WSA): A swarm intelligence algorithm for optimization problems–Part 1: Unconstrained optimization, *Appl Soft Comput*, **56** (2017) 520–540.
- 26 Baykasoğlu A & Akpınar Ş, Weighted Superposition Attraction (WSA): A swarm intelligence algorithm for optimization problems–Part 2: Constrained optimization, *App Soft Comput*, **37** (2017) 396–415.
- 27 Baykasoğlu A & Akpınar Ş, Enhanced superposition determination for weighted superposition attraction algorithm, *Soft Comput*, **24** (2020) 15015–15040.
- 28 Baykasoğlu A & Baykasoğlu C, Optimal design of truss structures using weighted superposition attraction algorithm, *Eng Comput*, **36** (2020) 965–979
- 29 Baykasoğlu A & Ozsoydan F B, Dynamic optimization in binary search spaces via weighted superposition attraction algorithm, *Expert Syst Appl*, **96** (2018) 157–174.
- 30 Baykasoğlu A, Ozsoydan F B & Senol M E, Weighted superposition attraction algorithm for binary optimization problems, *Oper Res*, **20** (2020) 2555–2581
- 31 Baykasoğlu A & Senol M E, Weighted superposition attraction algorithm for combinatorial optimization, *Exp Syst Appl*, **138** (2019) 112792.
- 32 Ozbakir L & Turna F, Clustering performance comparison of new generation meta-heuristic algorithms, *Knowl Based Syst*, **130** (2017) 1–16.
- 33 Baykasoğlu A, Golcuk I & Ozsoydan F B, Improving fuzzy c-means clustering via quantum-enhanced weighted superposition attraction algorithm, *Hacet J Math Stat*, **48(3)** (2019) 859–882.
- 34 Etter T, Schulz P, Weber M, Metz J, Wimpler M, Löffler J F & Uggowitzer P J, Aluminium carbide formation in interpenetrating graphite/aluminium composites, *Mater Sci Eng A*, **448(1-2)** (2007) 1–6.
- 35 Simsek D, Simsek I & Ozyurek D, Relationship between Al₂O₃ Content and wear behavior of Al+ 2% Graphite matrix composites, *Sci Eng Compos Mater*, **27(1)** (2020) 177–185.
- 36 Varga M, Winkelmann H & Badisch E, Impact of microstructure on high temperature wear resistance, *Proced Eng*, **10** (2011) 1291–1296.
- 37 Kumar N M, Kumaran S S & Kumaraswamidhas L A, Wear behaviour of Al 2618 alloy reinforced with Si₃N₄, AlN and ZrB₂ in situ composites at elevated temperatures, *Alex Eng J*, **55** (2016) 19–36.
- 38 Koraman E, Baydoğan M, Sayilgan S & Kalkanlı A, Dry sliding wear behaviour of Al–Fe–Si–V alloys at elevated temperatures, *Wear*, **322** (2015) 101–107.
- 39 Zhu H, Jar C, Song J, Zhao J, Li J & Xie Z, High temperature dry sliding friction and wear behavior of aluminum matrix composites (Al₃Zr+ α -Al₂O₃)/Al, *Tribol Int*, **48** (2012) 78–86.
- 40 Bharath V, Nagal M, Auradi V & Kori S A, Preparation of 6061Al-Al₂O₃ MMC's by stir casting and evaluation of mechanical and wear properties, *Proced Mater Sci*, **6** (2014) 1658–1667.
- 41 Uyyuru R K, Surappa M K & Brusethaug S, Tribological behavior of Al–Si–SiCp composites/automobile brake pad system under dry sliding conditions, *Tribol Int*, **40(2)** (2007) 365–373.
- 42 Çelik Y H, & Seçilmiş K, Investigation of wear behaviours of Al matrix composites reinforced with different B4C rate produced by powder metallurgy method, *Ad Powder Technol*, **28(9)** (2017) 2218–2224.
- 43 Şimşek D, Özyürek D & Salman S, Wear behaviors at different temperatures of ZrO₂ reinforced A356 matrix composites produced by mechanical alloying method, *Ind Lubr Tribol*, (2022) <https://doi.org/10.1108/ILT-10-2021-0416>
- 44 Daouda A, abou-elkhair M T & Rohatgi P, Wear and friction behavior of near eutectic Al–Si+ZrO₂ or WC Particle Composites, *Compo Sci Technol*, **64** (2004) 1029–1040.
- 45 Natarajan S, Narayanasamy R, Kumares S P, Dinesh G, Anil B & Sivaprasad K, Sliding wear behaviour of Al 6063/TiB₂ in situ composites at elevated temperatures, *Mater Des*, **30** (2009) 2521–2531.

- 46 Kim T H, Maruta I & Sugie T, A simple and efficient constrained particle swarm optimization and its application to engineering design problems, *Proc Inst Mech Eng Part C*, **224(2)** (2010) 389–400.
- 47 Baykasoglu A, Design optimization with chaos embedded great deluge algorithm, *Appl Soft Comput*, **12(3)** (2012) 1055–1067.
- 48 Stojanović B, Gajević S, Kostić N, Miladinović S & Vencl A, Optimization of parameters that affect wear of A356/Al₂O₃ nanocomposites using RSM, ANN, GA and PSO methods, *Ind Lubr Tribol* (2022) <https://doi.org/10.1108/ILT-07-2021-0262>
- 49 Rana R S, Purohit R, Kumar Sharma A & Rana S, Optimization of wear performance of Aa 5083/10 Wt.% Sicp composites using Taguchi method, *Proced Mater Sci*, **6** (2014) 503–511.
- 50 Prakash J U, Ananth S, Sivakumar G & Moorthy T V, Multi-objective optimization of wear parameters for aluminium matrix composites (413/B4C) using grey relational analysis, *Mater Today: Proc*, **5(2)** (2018) 7207–7216.